Journal of Hazardous Materials 164 (2009) 542–548

Contents lists available at ScienceDirect

Journal of Hazardous Materials

journal homepage: www.elsevier.com/locate/jhazmat

Characterization and activity of Pd-modified TiO_2 catalysts for photocatalytic oxidation of NO in gas phase

Zhongbiao Wu, Zhongyi Sheng, Yue Liu*, Haiqiang Wang, Nian Tang, Jie Wang

Department of Environmental Engineering, Zhejiang University, Hangzhou 310027, PR China

ARTICLE INFO

Article history:
Received 28 May 2008
Received in revised form 12 August 2008
Accepted 12 August 2008
Available online 19 August 2008

Keywords:
Photocatalytic oxidation
NO
TiO_2
Palladium doping
Hydroxyl groups

ABSTRACT

Pd-modified TiO_2 prepared by thermal impregnation method was used in this study for photocatalytic oxidation of NO in gas phase. The physico-chemical properties of Pd/TiO_2 catalysts were characterized by X-ray diffraction analysis (XRD), Brunauer-Emmett-Teller measurements (BET), X-ray photoelectron spectrum analysis (XPS), transmission electron microscopy (TEM), high resolution-transmission electron microscopy (HR-TEM), UV–vis diffuse reflectance spectra (UV–vis DRS) and photoluminescence spectra (PL). It was found that Pd dopant existed as PdO particles in as-prepared photocatalysts. The results of PL spectra indicated that the photogenerated electrons and holes were efficiently separated after Pd doping. During in situ XPS study, it was found that the content of hydroxyl groups on the surface of Pd/TiO_2 increased when the catalyst was irradiated by UV light, which could result in the improvement of photocatalytic activity. The activity test showed that the optimum Pd dopant content was 0.05 wt.%. And the maximum conversion of NO was about 72% higher than that of P25 when the initial concentration of NO was 200 ppm, which showed that Pd/TiO_2 photocatalysts could be potentially applied to oxidize higher concentration of NO.

1. Introduction

Nitrogen oxides (NOx) exhausted from stationary sources and mobile sources can cause ozone depletion, photochemical smog and the acid deposition [1,2]. With the development of society and industry, increasing consumption of fossil fuels has resulted in large emissions of NOx. Among the NOx emitted from stationary combustion sources, more than 90% of NOx is nitric oxide (NO). Wet scrubbing method, which is widely used for sulfur dioxide (SO_2) removal, promises to be less expensive than other methods for NOx removal, such as combustion modification, selective catalytic reduction (SCR) and selective noncatalytic reduction (SNCR) [3–6]. In order to remove NOx by wet scrubbing methods, it is necessary to oxidize NO to more soluble nitrogen dioxide (NO_2) or dinitrogen pentoxide (N_2O_5) in either gas or liquid phase [7,8].

The photocatalytic oxidation using titanium dioxide (TiO_2) as photocatalyst has been shown to be a relatively cheap and effective process to convert NO to NO_2 in gas phase [9–11]. When irradiated by wavelengths less than 380 nm on TiO_2, electrons will be excited from the valence to the conduction band, generating electron–hole pairs that can recombine or initiate redox reactions. Holes are trapped by water (H_2O) or hydroxyl groups (OH^-) adsorbed on the surface to generate hydroxyl radicals ($OH^\bullet$). Electrons reduce adsorbed oxygen to yield superoxide ions ($O_2^{\bullet-}$). It is well known that $OH^\bullet$ and $O_2^{\bullet-}$ groups on TiO_2 surface play important roles in NO adsorption and oxidation process [12]. Eqs. (1)–(8) in the following could reveal the formation of $OH^\bullet$ and $O_2^{\bullet-}$ groups and NO oxidation mechanism.

$$TiO_2 + h\nu \rightarrow e_{CB}^- + h_{VB}^+ \quad (1)$$

$$h_{VB}^+ + H_2O_{ads} \rightarrow HO_{ads}^\bullet + H^+ \quad (2)$$

$$h_{VB}^+ + HO_{ads}^- \rightarrow HO_{ads}^\bullet \quad (3)$$

$$e_{CB}^- + O_{2ads} \rightarrow O_{2ads}^{\bullet-} \quad (4)$$

$$NO + HO_{ads}^\bullet \rightarrow HNO_2 \quad (5)$$

$$HNO_2 + HO_{ads}^\bullet \rightarrow NO_2 + H_2O \quad (6)$$

$$NO_2 + HO_{ads}^\bullet \rightarrow HNO_3 \quad (7)$$

$$NO + O_{2ads}^{\bullet-} \rightarrow NO_3^- \quad (8)$$

It is reported that there are three states during photocatalytic oxidation process of NO [13,14]. At the initial state, the oxidation product is HNO_2. And then in the transient state, oxidation of HNO_2 to NO_2 and subsequent oxidation of NO_2 to HNO_3 occur. Once the catalyst is saturated with HNO_3, the steady state reaches and the oxidation

* Corresponding author. Tel.: +86 571 87953088; fax: +86 571 87953088.
E-mail address: yueliu@zju.edu.cn (Y. Liu).

0304-3894/$ – see front matter © 2008 Elsevier B.V. All rights reserved.
doi:10.1016/j.jhazmat.2008.08.028

reaction can only go as far as NO_2. The nitrogen mass balance about NO and NO_2 is established at the steady state.

Our previous study showed that TiO_2 coated on the woven glass fabric was effective for the oxidation of NO at low concentration [14,15]. However, in order to oxidize higher concentration of NO, further improvement of the characteristics of the photocatalysts is required. The recombination probability between photogenerated electrons and holes is a major factor limiting the photocatalytic activity [16,17]. Several approaches have been adopted to enhance the photocatalytic activity of TiO_2 such as its preparation as nano-sized particles [15,18], doping and coating with metals [19–21] or modifying with other semiconductors [22,23].

Among these above-mentioned methods, it has been shown that modification of the TiO_2 surface with noble metals will be one of the most successful ways to improve the photocatalytic efficiency. Doped-Pd on TiO_2 has been applied in the photocatalytic oxidation of organic pollutants [24,25]. It is proposed that Pd species facilitate the photoexcited electrons transfer and hence retard recombination of photogenerated electron and hole. Due to these good properties, Pd-modified TiO_2 was used for the gas-phase photocatalytic oxidation of NO in our previous study [26]. It was found that NO oxidation on Pd-modified TiO_2 showed very different behaviors from that on pure TiO_2.

As an extension work of our previous study, full characterizations of Pd/TiO_2 prepared by thermal impregnation method were carried out by X-ray diffraction analysis (XRD), Brunauer-Emmett-Teller measurements (BET), X-ray photoelectron spectrum analysis (XPS), transmission electron microscopy (TEM), high resolution-transmission electron microscopy (HR-TEM), UV–vis diffuse reflectance spectra (UV–vis DRS) and photoluminescence spectra (PL). An in situ XPS experiment was conducted to examine the changes in valance states of Pd and content of hydroxyl groups on the surface of Pd/TiO_2 under UV irradiation, which could be related to the photocatalytic oxidation performance during the reaction process. Finally, the photocatalytic activity of Pd/TiO_2 for the oxidation of NO at high concentrations (80–310 ppm) was investigated.

2. Materials and methods

2.1. Catalyst preparation

Commercial TiO_2 Degussa P25 was used as the photocatalyst and the precursor. The photocatalysts were prepared by dispersal of 8.0 g TiO_2 powder into 100 ml Pd^{2+}/HCl solution (4–160 mg/100 ml) to obtain Pd loading of 0.02–1 wt.%. The slurry was then stirred for 48 h. After that, it was heated at 373 K for 12 h followed by calcination at 673 K for 1 h in air.

2.2. Catalyst characterization

XRD patterns were obtained by a Rigaku D/Max RA diffractometer with Cu Kα radiation at 40 kV and 150 mA, at an angle of 2θ from 20° to 80°. BET surface areas (S_{BET}) were determined using N_2 physisorption at 77 K, with a Micromeritics ASSP 2020 equipment. Surface element analysis was carried out by XPS using a Thermo ESCALAB 250 instrument with Al Kα radiation ($h\nu$ = 1486.6 eV) at 150 W. The signal of adventitious carbon (a binding energy of 284.8 eV) has been used to calibrate the binding energy scale for XPS measurements. The morphology, structure and grain size of Pd-modified TiO_2 were examined by TEM and HR-TEM with a JEM-2010 instrument. The crystal UV–vis diffuse reflectance spectra of the samples in the wavelength range of 200–800 nm were measured by a Purkinje TV-1901 spectrophotometer with an integrating sphere, and $BaSO_4$ was used as a reference sample. PL spectra were measured at room temperature using a Fluorolog-3-Tau fluorospectrophotometer with a Xe lamp as the excitation light source.

2.3. Photocatalytic reaction

The method of photocatalyst immobilization was carried out by the dip-coating method [14]. The modified TiO_2 (8 g) was carefully grinded and added to 100 ml deionized water under vigorous stirring. Then the woven glass fabric (pretreatment: 500 °C for 1 h) with an area of 4 cm × 80 cm was dipped into the TiO_2 suspension and the catalyst was coated on. In all experiments, the weight of catalyst coated was kept to be 0.5 g ± 10%.

The experiment setup and operating conditions for photocatalytic activity tests were the same as that in our previous reports [14,15]. All the photocatalytic activity experiments were carried out in a continuous setup. The setup consisted of a gas supply, reactor and analytical system. An air compressor, a NO cylinder (10,000 ppm, diluted by N_2) and a N_2 cylinder (99.9%) were supplied as gas sources. By varying the flow rate of one stream air bubbled through a gas wash bottle, the humidity could be adjusted. The air, NO, and N_2 streams were mixed to obtain the desired concentration (NO: 80–310 ppm, relative humidity: 75%). The flow rate of the gas was 2.0 l/min and the space time was 10 s. Photocatalytic experiments were carried out in a 340 ml cylindrical Pyrex glass reactor. The immobilized catalyst was set into the reactor with a "Z" type. The irradiation source was an Hg-arc lamp (125 W, Philips) located outside the reactor. The wavelength of the Hg-arc lamp varied in the range from 300 to 400 nm with the maximum light intensity at 365 nm. The reaction temperature in the reactor was 80 ± 5 °C, from the irradiation of the lamp. NO, NO_2 and O_2 were analyzed with a flue gas analyzer (Kane International Ltd., Model KM-9106). The relative humidity was measured with a relative humidity analyzer (Testo Co. Ltd., Model 605-H1).

Blank tests were conducted with the Hg-arc turned on but without the photocatalyst using 80–310 ppm inlet NO, at 80 ± 5 °C. The variation of the NO concentration could not be observed within 120 min irradiation. Furthermore, there was no change of the NO concentration when the Hg-arc lamp was turned off and the catalyst was present in the reactor.

3. Results and discussion

3.1. Crystal phase and surface composition

The XRD spectra of photocatalysts with increasing Pd content from 0 to 1 wt.% are shown in Fig. 1. Peaks marked "A" and "R" correspond to anatase and rutile phases, respectively. From Fig. 1, all photocatalysts displayed a mixture of anatase and rutile, and no Pd containing species were observed. The average crystalline sizes of anatase and rutile were obtained from XRD data with the Scherrer equation [27]. The phase contents of the samples could be calculated with the following equation [28]:

$$f_R = \left[1 + 0.79\left(\frac{I_A}{I_R}\right)\right]^{-1} \quad (9)$$

where f_R is the weight fraction of rutile phase in the sample, and I_A, I_R are the X-ray intensities of the anatase (1 0 1) and rutile (1 1 0) diffraction peaks, respectively. It was found that there were little changes in the crystalline phase composition, phase size and specific surface area for TiO_2 after Pd doping (Table 1).

The element compositions on the surface of Pd/TiO_2 were determined by XPS high-resolution scans over C 1s, O 1s, Cl 2p, Ti 2P and Pd 3d spectra regions as shown in Fig. 2. High-resolution scan over Pd 3d peaks showed that the binding energy of Pd $3d_{5/2}$ was

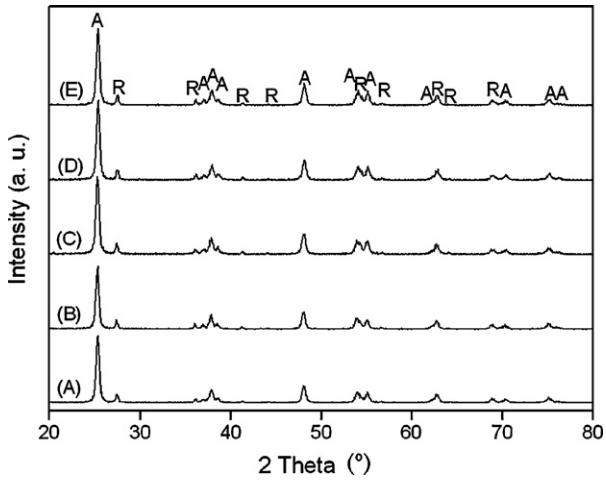

Fig. 1. XRD patters of catalysts with P25 (A) and different Pd dopant content of 0.02 wt.% (B), 0.05 wt.% (C), 0.1 wt.% (D), and 1 wt.% (E).

Table 1
Physical and morphological properties of the photocatalysts

Catalyst	S_{BET} ($m^2\ g^{-1}$)	Rutile fraction (%)	Diameter[a] of TiO_2 (nm)
P25	46	7.75	20.3 (A); 31.2 (R)
0.02 wt.% Pd/TiO_2	53	7.60	20.6 (A); 31.9 (R)
0.05 wt.% Pd/TiO_2	46.4	9.37	24.0 (A); 33.6 (R)
0.1 wt.% Pd/TiO_2	52.3	10.05	21.3 (A); 33.5 (R)
1 wt.% Pd/TiO_2	50.1	9.99	21.3 (A); 33.6 (R)

[a] (A) stands for anatase and (R) for rutile.

336.06 eV, which indicated that Pd loaded on the catalysts existed as Pd^{2+}.

The morphology of Pd-modified TiO_2 powders was further investigated by TEM and HR-TEM images as shown in Fig. 3. TEM image (Fig. 3a) confirmed the presence of Pd deposits on the surface of Degussa P25. As shown in Fig. 3a, Pd deposits were well dispersed on many of the TiO_2 particles and had the diameters predominantly ranged from 3 to 5 nm. From the HR-TEM image illustrated in Fig. 3b, clear lattice fringes could be observed for Pd-modified TiO_2 particles. The observed spacing between the lattice planes of the sample was obtained as 0.352 nm for (1 0 1) plane of the anatase crystal (Fig. 3b as shown by the left arrowhead) [29]. Another observed spacing between the lattice planes was observed

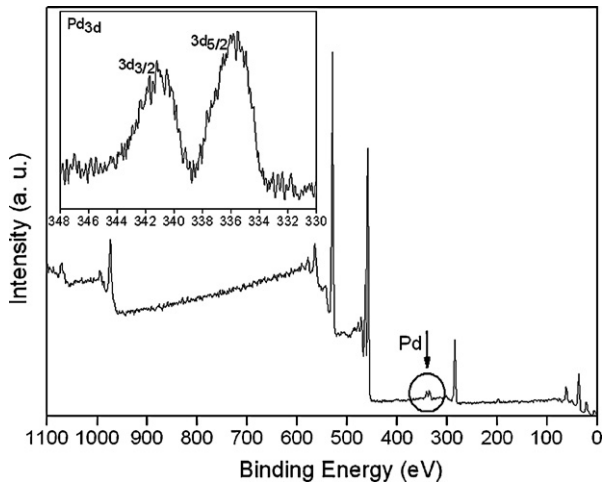

Fig. 2. XPS scan over the surface of 1 wt.% Pd/TiO_2. The Pd 3d line is plotted in the inset.

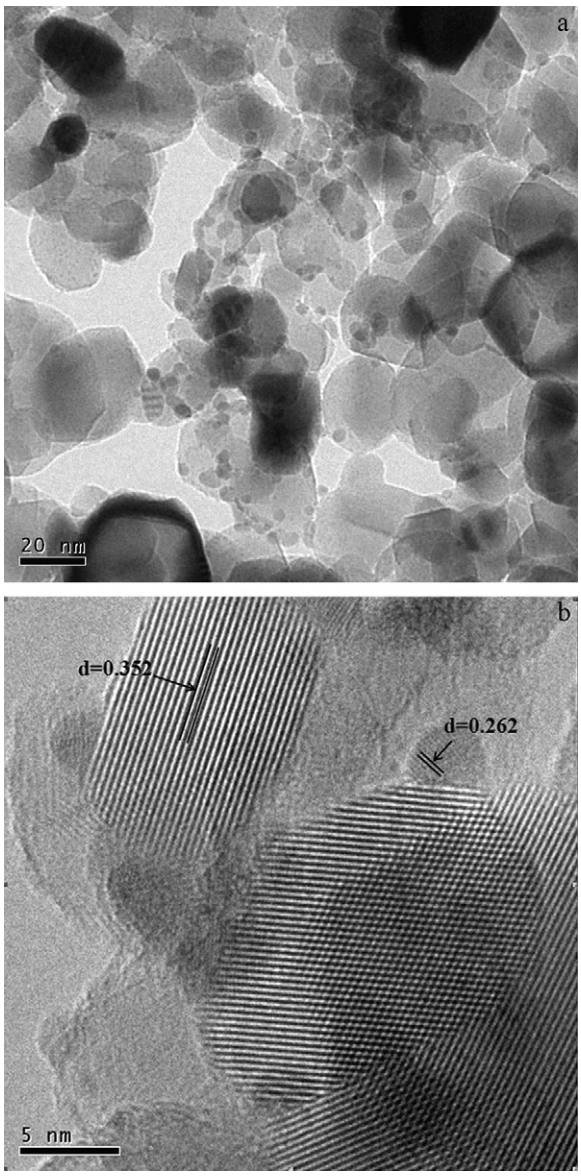

Fig. 3. TEM (a) and HR-TEM (b) images of 1 wt.% Pd/TiO_2.

as about 0.262 nm, matching the (1 0 1) plane of PdO crystal, which confirmed that Pd dopant exists as PdO [30].

3.2. Optical absorption and PL characteristics

Fig. 4 shows the UV–vis diffuse reflectance spectra for the photocatalysts prepared from P25 with different Pd deposited amount. The spectra of P25 consisted of a single and broad intense absorption around 400 nm due to a charge-transfer transition between the lattice oxygen ligands (O^{2-}) and a central titanium ion (Ti^{4+}) with octahedral coordination. In the spectra of Pd/TiO_2, almost similar absorption intensity was shown at wavelength shorter than 385 nm, which could be accounted for the intrinsic band gap absorption of pure anatase TiO_2 (3.2 eV). A broad band between 450 and 550 nm centered at 470 nm could be observed in the absorption spectra of Pd/TiO_2 owing to a d–d transition of PdO particles [31]. And the background absorption intensity at wavelength longer than 400 nm was enhanced with the increasing amount of Pd.

Photoluminescence (PL) emission spectra have been used to study the transfer behavior of the photogenerated electrons and

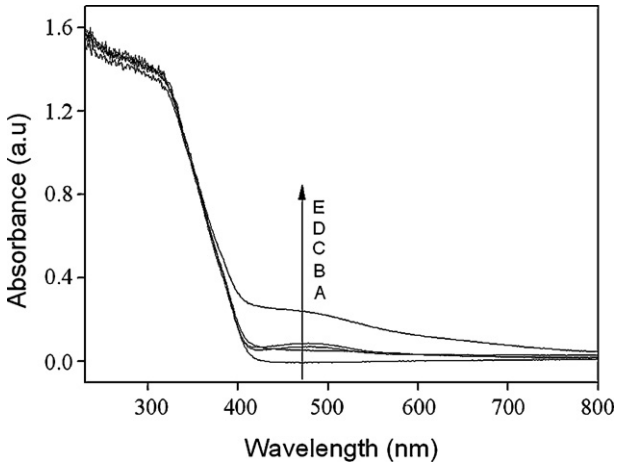

Fig. 4. UV–vis diffuse reflectance spectra of the catalysts with P25 (A) and different Pd dopant content of 0.02 wt.% (B), 0.05 wt.% (C), 0.1 wt.% (D), and 1 wt.% (E).

holes and understand the separation and recombination of photogenerated charge carriers [32]. In order to investigate the photoelectric properties of Pd/TiO_2, the PL spectra were detected for the different samples exited at 300 nm at room temperature as shown in Fig. 5. The PL intensity greatly decreased with the increase of the Pd dopant content. It is known that the intensity of the emission from the TiO_2 particles is strongly dependent on the surface treatment of the TiO_2 particles [33]. PdO particles deposited on the surface could act as trapping sites to capture photogenerated electrons from TiO_2 conduction band, separating the photogenerated electron-hole pairs. Therefore, the recombination rate of photogenerated electrons and holes was retarded, leading to the reduction of PL signal decrease.

3.3. In situ XPS study

An in situ XPS study was conducted to examine the changes in the compositions of chemical species on the surface of Pd/TiO_2 under UV irradiation. 1 wt.% Pd/TiO_2 was firstly placed in the dark overnight before XPS scans. Then, the sample was irradiated by UV light. XPS scans were performed after 0.5 and 3 h irradiation.

Fig. 6a shows the Pd 3d peaks of Pd/TiO_2 in the dark and after 0.5 and 3 h irradiation. The peak of Pd $3d_{5/2}$ was shifted from 336.06 eV (Fig. 6a, A) to 335.12 eV (Fig. 6a, C), which clearly suggested that a portion of Pd^{2+} on the surface of Pd/TiO_2 was reduced to metallic Pd (peak at 334.9 eV) under the UV irradiation. When irradiated by UV light with wavelength less than 380 nm, electron–hole pairs on TiO_2 were generated. PdO particles dispersed on TiO_2 surface were populated with the generated electrons, resulting in the transformation of Pd^{2+} to Pd^0 (see Eq. (10)).

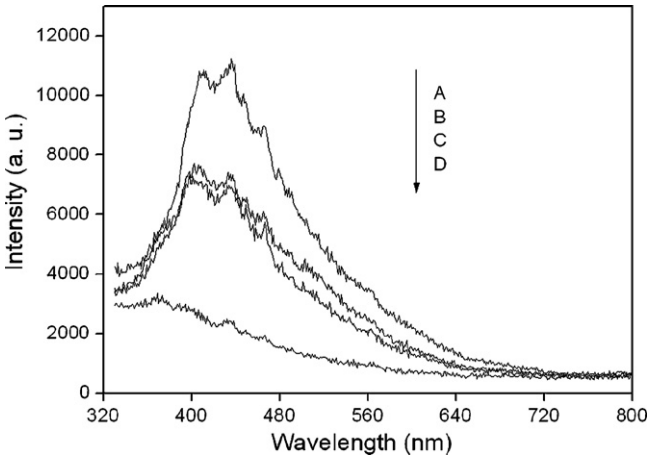

Fig. 5. PL spectra of photocatalysts with different Pd deposited amounts of 0 (A), 0.05 wt.% (B), 0.1 wt.% (C) and 1 wt.% (D) at room temperature after the excitation at 300 nm.

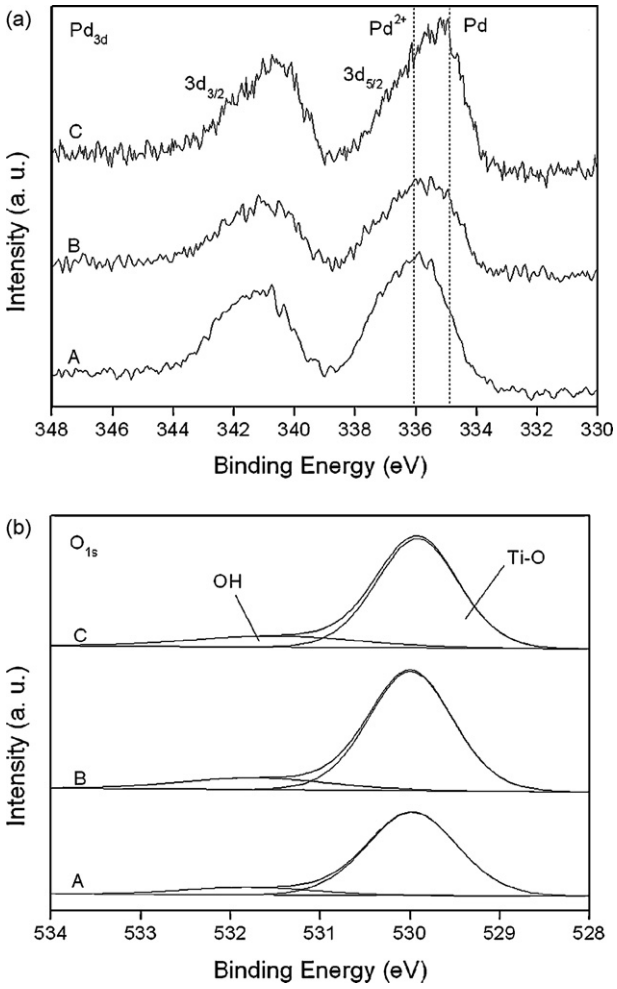

Fig. 6. Comparison of XPS high-resolution scans over Pd 3d (a) and O 1s (b) peaks on 1 wt.% Pd/TiO_2 in the dark (A) and after 0.5 h (B), 3 h (C) irradiation. UV irradiation source: He I ($h\nu$ = 21.2 eV), vacuum: $(2–3) \times 10^{-7}$ Pa.

$$Pd^{2+} + 2e_{CB}^{-} \rightarrow Pd \quad (10)$$

Fig. 6b shows the O 1s peaks of Pd/TiO_2 before and after UV irradiation. The peak of O 1s could be well fitted as a combination of Ti–O (peak at 529.9) and the OH^- groups (peak at 531.8) [34]. The main contribution was attributed to Ti–O in TiO_2 crystal lattice, and the other minor peak was ascribed to the Ti–OH on the surface of Pd/TiO_2. Table 2 lists the results of curve fitting of XPS spectra for Pd/TiO_2 powders before and after UV irradiation. It could be seen from Table 2 that the content of oxygen element on the surface decreased and the fraction of hydroxyl groups on the surface of Pd/TiO_2 had an obvious increase after 3 h irradiation. The content of oxygen element decreased from 70.5% to 68.8% after 3 h irradiation, which might be explained by the fact that surface oxygen atoms on TiO_2 could be oxidized to oxygen molecules by photogenerated holes, leaving oxygen vacancies [35]. After 3 h irradiation, the fraction of hydroxyl groups on the surface increased from 11.5% to 17.2%, which may be related to the destruction of Ti–O–Ti and the formation of Ti–OH on the surface of TiO_2 crystallites. It was

Table 2
Results of curve fitting of high-resolution XPS spectra for the O 1s and Pd $3d_{5/2}$ peaks of 1 wt.% Pd/TiO_2 samples in the dark (A) and after 0.5 h (B), 3 h (C) irradiation

Sample	O 1s			Pd $3d_{5/2}$
	O 1s	O 1s (Ti–O)	O 1s (OH)	
A				
E_b (eV)		529.98	531.8	336.06
r_i (%)	70.5	88.5	11.5	0.61
B				
E_b (eV)		529.94	531.68	335.49
r_i (%)	70.4	85.4	14.6	0.60
C				
E_b (eV)		529.92	531.49	335.12
r_i (%)	68.8	82.8	17.2	0.63

UV irradiation source: He I ($h\nu$ = 21.2 eV), vacuum: $(2–3) \times 10^{-7}$ Pa.

indicated by Nakamura et al. [36–39] that the bridged Ti–O–Ti site on the surface could be broken by a nucleophilic attack of an H_2O molecule to a surface-trapped hole at the surface lattice O site (see Eqs. (11) and (12)).

$$\text{Ti–O–Ti} + h_{VB}{}^{+} + H_2O \rightarrow \text{Ti–O·HO–Ti} + H^{+} \quad (11)$$

$$\text{Ti–O·HO–Ti} + h_{VB}{}^{+} \rightarrow \text{Ti–O–O–Ti} + H^{+} \quad (12)$$

Then the Ti–O–O–Ti site further reacted with water molecular adsorbed on the surface of TiO_2 to form Ti–OH [37] shown as Eq. (13).

$$\text{Ti–O–O–Ti} + H_2O \rightarrow [\text{Ti–OOH HO–Ti}] + H^{+} \quad (13)$$

However, the changes of hydroxyl groups could not be observed on TiO_2 without Pd modification, which indicated that the recombination rate between photogenerated holes and electrons was fast and few holes could be utilized to oxidize surface oxygen atoms. This result proved that photogenerated electrons and holes could be efficiently separated after Pd doped on TiO_2. The increase of hydroxyl groups on the surface could enhance the photocatalytic activity of Pd/TiO_2 over the oxidation of NO because of their important roles in NO adsorption and oxidation process shown as Eqs. (3)–(7).

3.4. Behavior of photocatalytic oxidation

Fig. 7 shows the variations of the conversion of NO with irradiation time over P25 and 0.05 wt.% Pd/TiO_2 catalysts in humidified environment. The NO conversion over P25 decreased and approached a steady state after 300 min of irradiation. Similar results could be found in the literatures [13–15]. It is generally considered that the high initial conversion is the result of chemisorption [13]. It is indicated from Fig. 7 that the evolution of the activity vs. irradiation time for Pd/TiO_2 is different from that for P25. For Pd-modified TiO_2 catalysts, the NO conversion increased with irradiation time and tended to be a constant value. With 0.05 wt.% Pd/TiO_2 catalyst, the minimum conversion (43.9%) was observed at the beginning of reaction. And after 1200 min of irradiation, the conversion reached the maximum value of 87.2%.

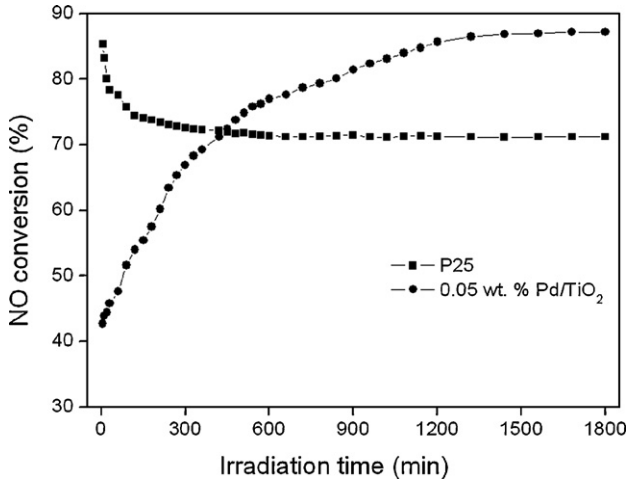

Fig. 7. Variations of NO conversion efficiency with irradiation time for P25 and 0.05 wt.% Pd/TiO_2. *Conditions*: 125 W Hg-arc, 80 °C, 75% RH, 10 s space time, 21% O_2 concentration and 80 ppm initial NO concentration.

In our previous report, it had been indicated that the formation of Pd^{4+} could be considered as one possible reason of different behavior between P25 and Pd/TiO_2 [26]. However, the changes in the compositions of hydroxyl groups on the surface of Pd/TiO_2 under UV irradiation could be another possible reason. Under UV irradiation, $OH^{\bullet}$ radicals could be produced from OH^- groups on the surface of TiO_2 oxidization by photogenerated holes. Eq. (3) reveals the formation of $OH^{\bullet}$ radicals, which have been detected by ESR spin trapping [40–42]. Eqs. (5)–(7) indicate that $OH^{\bullet}$ radicals play important roles in NO adsorption and oxidation process. Therefore, the enhanced photocatalytic oxidation of NO could be promoted by the increase in the concentration of surface OH^- groups. However, due to lack of the electron trapping sites like Pd species, the recombination rate between photogenerated holes and electrons was fast on P25 without Pd modification and few holes could be utilized to oxidize surface oxygen atoms. Thus the increase of OH^- groups could not occur on TiO_2 without Pd modification. For the photocatalytic oxidation of NO on P25, $OH^{\bullet}$ radicals participating in NO adsorption and reaction were mainly from adsorbed H_2O but not surface OH^- groups.

During the initial state of the reaction, photogenerated electrons were transferred from TiO_2 conduction band to the Pd^{2+} and a portion of Pd^{2+} could be reduced to Pd^0 (see Eq. (10)). And the OH^- groups would be formed from TiO_2 surface oxygen atoms oxidation by photogenerated holes, which has been indicated by the in situ XPS study as shown in Fig. 6 and Table 2. $OH^{\bullet}$ was scarily formed to participate in NO adsorption and oxidation reaction in the initial state, which resulted in the low conversion as shown in Fig. 7. As the reaction going on, OH^- groups on the surface of TiO_2 could act as photogenerated holes trapping sites. It would let more $OH^{\bullet}$ radicals to participate in the photocatalytic reaction, and a rise in conversion could be observed (see Fig. 7).

3.5. Photocatalytic activity

Fig. 8 shows the NO conversion efficiency on Pd-modified TiO_2 after 1200 min of irradiation with inlet NO concentration of 200 ppm. A series of Pd dopant contents, such as 0.02, 0.05, 0.1, 0.2 and 1 wt.%, were chosen to investigate the relationship between the Pd contents and the photocatalytic activities of Pd/TiO_2. It can be seen from Fig. 8 that the photocatalytic oxidation activity of NO greatly improves with the increase of Pd dopant content from 0 to 0.05 wt.%, then decreases with the further increasing of Pd loading. Therefore, the optimum Pd dopant content was 0.05 wt.%. The highest conversion (72.2%) occurred on 0.05 wt.% Pd/TiO_2, which was about 72% higher than that with P25 (42%). From the above-mentioned PL results (see Fig. 5), it was indicated that the separation of the photogenerated electrons and holes was promoted after Pd doping. Moreover, the increase in the concentration of surface OH^- groups under UV irradiation on Pd/TiO_2 could result in more $OH^{\bullet}$ radicals to participate in photocatalytic oxidization of NO. However, the enhancement of activity for Pd modification decreased when the Pd doping content was higher

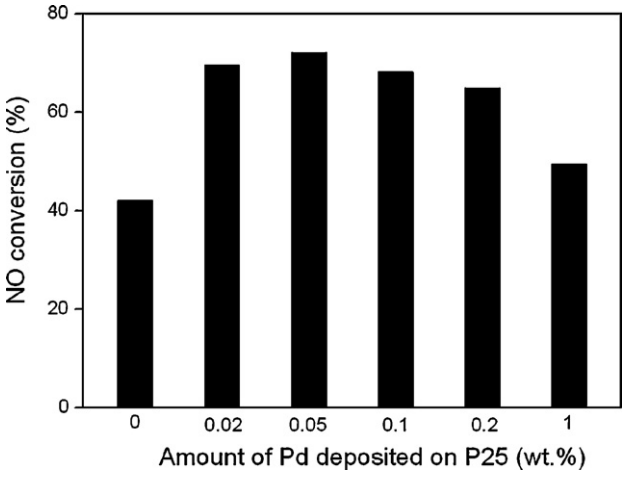

Fig. 8. Comparison of different Pd deposited content based on P25 in photocatalytic oxidation of NO after 1200 min of irradiation. *Conditions*: 125 W Hg-arc, 80 °C, 75% RH, 10 s space time, 21% O_2 concentration and 200 ppm initial NO concentration.

than 0.05 wt.%. It can be explained by the fact that the surface of TiO_2 was covered by too much Pd dopant so that it could not be irradiated efficiently, which reduced the apparent photo-quantum yield of photocatalytic process.

Fig. 9 shows the NO conversion efficiency on 0.05 wt.% Pd/TiO_2 and P25 with different inlet concentration of NO. It can be shown in Fig. 9 that the photocatalytic oxidation efficiency of NO both decline with the increase of NO concentration. For P25, the conversion of NO was 72.4% when the inlet concentration was 85 ppm, and decreased to 25.8% when the inlet concentration reached 310 ppm. It had been reported that the reaction rate which placed on the Degussa P25 was limited by the Langmuir–Hinshelwood model, where the reaction was first-order at low concentrations and zero-order at high concentrations [13,14]. However, the photocatalytic activity of 0.05 wt.% Pd/TiO_2 performed well at higher concentration of NO. The conversion of NO (87.2%) was about 1.13 times that of P25 (72.4%) at inlet NO concentration of 85 ppm, while the conversion (60.3%) was about 2.34 times that of P25 (25.8%) at 310 ppm. The reason could be considered as the increasing adsorption sites of NO on surface of TiO_2 after Pd doping [43].

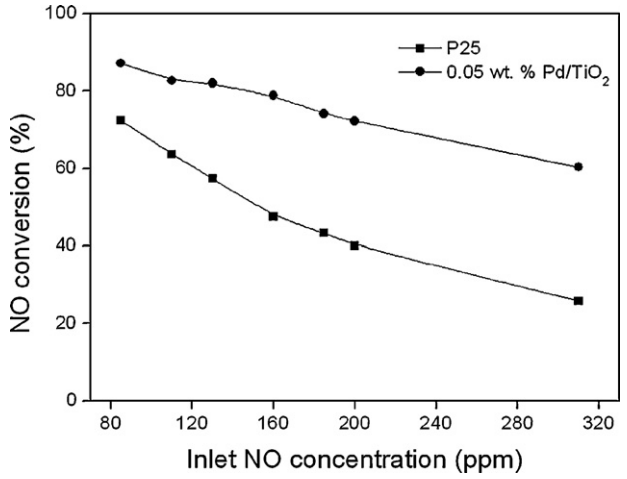

Fig. 9. Effect of NO conversion efficiency with initial NO concentration after 1200 min irradiation using P25 and 0.05 wt.% Pd/TiO_2. *Conditions*: 125 W Hg-arc, 80 °C, 75% RH, 10 s space time and 21% O_2 concentration.

4. Conclusions

In this study, Pd-modified TiO_2 photocatalysts were prepared by thermal impregnation method and used for the photocatalytic oxidation of NO. The experimental results showed that the optimum Pd dopant content was 0.05 wt.%. With Pd dopant content of 0.05 wt.%, the concentration of NO could reach 72.2% with inlet NO concentration of 200 ppm, which was 72% higher than that of P25. Full characterizations of Pd/TiO_2 were also conducted to investigate the relationship between the physico-chemical properties and photocatalytic activity. PL spectra identified that the doping of Pd on TiO_2 could inhibit the recombination of photogenerated electrons and holes. During in situ XPS study, it was found that metallic Pd^0 could be formed from the reduction of Pd^{2+} by photogenerated electrons and the content of OH^- groups on the surface increased because of the oxygen atoms oxidation by holes. The increase content of OH^- groups could be considered as one of the reasons for its high photocatalytic activity and different oxidation behavior from P25.

Acknowledgements

This work was financially supported by the National High-Tech Research and Development Program (863) of China (2007AA061701), the Excellent Young Teacher Support Program of Zhejiang University (2007) and the New Century Excellent Scholar Program of Ministry of Education of China (NCET-04-0549).

References

[1] A. Farrell, Multi-lateral emission trading: lessons from inter-state NOx control in the United States, Energy Policy 29 (2001) 1061–1072.
[2] T. Castro, S. Madronich, S. Rivale, A. Muhlia, B. Mar, The influence of aerosols on photochemical smog in Mexico City, Atmos. Environ. 35 (2001) 1765–1772.
[3] C.D. Cooper, F.C. Alley, Air Pollution Control: A Design Approach, Waveland Press, Prospect Heights, IL, 1994.
[4] X.L. Tang, J.M. Hao, W.G. Xu, J.H. Li, Low temperature selective catalytic reduction of NOx with NH_3 over amorphous MnOx catalysts prepared by three methods, Catal. Commun. 8 (2007) 329–334.
[5] J.M. Beer, Combustion technology developments in power generation in response to environmental challenges, Prog. Energy Combust. Sci. 26 (2000) 301–327.
[6] A.M. Efstathiou, K. Fliatoura, Selective catalytic reduction of nitric oxide with ammonia overV_2O_5/TiO_2 catalyst: a steady-state and transient kinetic study, Appl. Catal. B: Environ. 6 (1995) 35–39.
[7] Y.S. Mok, Absorption–reduction technique assisted by ozone injection and sodium sulfide for NOx removal from exhaust gas, Chem. Eng. J. 118 (2006) 63–67.
[8] Y.G. Adewuyi, S.O. Owusu, Aqueous absorption and oxidation of nitric oxide with oxone for the treatment of tail gases: process feasibility, stoichiometry, reaction pathways, and absorption rate, Ind. Eng. Chem. Res. 42 (2003) 4084–4100.
[9] T. Ibusuki, K. Takeuchi, Removal of low concentration of nitrogen oxides through photoassisted heterogeneous catalysis, J. Mol. Catal. 88 (1994) 93–102.
[10] C.H. Ao, S.C. Lee, C.L. Mak, L.Y. Chan, Photodegradation of volatile organic compounds (VOCs) and NO for indoor air purification using TiO_2: promotion versus inhibition effect of NO, Appl. Catal. B 42 (2003) 119–129.
[11] C.H. Ao, S.C. Lee, Enhancement effect of TiO_2 immobilized on activated carbon filter for the photodegradation of pollutants at typical indoor air level, Appl. Catal. B 44 (2003) 191–205.
[12] J.C.S. Wu, Y.T. Cheng, In situ FTIR study of photocatalytic NO reaction on photocatalysts under UV irradiation, J. Catal. 237 (2006) 393–404.
[13] S. Devahasdin, C. Fan Jr., K. Li, D.H. Chen, TiO_2 photocatalytic oxidation of nitric oxide: transient behavior and reaction kinetics, J. Photochem. Photobiol. A 156 (2003) 161–170.
[14] H.Q. Wang, Z.B. Wu, W.R. Zhao, B.H. Guan, Photocatalytic oxidation of nitrogen oxides using TiO_2 loading on woven glass fabric, Chemosphere 66 (2007) 185–190.
[15] Z.B. Wu, H.Q. Wang, Y. Liu, Z.L. Gu, Photocatalytic oxidation of nitric oxide with immobilized titanium dioxide films synthesized by hydrothermal method, J. Hazard. Mater. 151 (2008) 17–25.
[16] A.L. Linsebigler, G.Q. Lu, J.T. Yates Jr., Photocatalysis on TiO_2 surfaces: principles, mechanisms, and selected results, Chem. Rev. 95 (1995) 735–758.
[17] M.R. Hoffmann, S.T. Martin, W. Choi, D.W. Bahnemann, Environmental applications of semiconductor photocatalysis, Chem. Rev. 95 (1995) 69–96.

[18] J.G. Yu, H.G. Yu, B. Cheng, M.H. Zhou, X.J. Zhao, Enhanced photocatalytic activity of TiO_2 powder (P25) by hydrothermal treatment, J. Mol. Catal. A 253 (2006) 112–118.
[19] H. Einaga, T. Ibusuki, S. Futamura, Improvement of catalyst durability by deposition of Rh on TiO_2 in photooxidation of aromatic compounds, Environ. Sci. Technol. 38 (2004) 285–289.
[20] E.A. Kozlova, A.V. Vorontsov, Noble metal and sulfuric acid modified TiO_2 photocatalysts: mineralization of organophosphorous compounds, Appl. Catal. B 63 (2006) 114–123.
[21] X.F. You, F. Chen, J.L. Zhang, M. Anpo, A novel deposition precipitation method for preparation of Ag-loaded titanium dioxide, Catal. Lett. 102 (2005) 247–250.
[22] S.G. Yang, X. Quan, X.Y. Li, Y.Z. Liu, S. Chen, G.H. Chen, Preparation, characterization and photoelectrocatalytic properties of nanocrystalline Fe_2O_3/TiO_2, ZnO/TiO_2, and $Fe_2O_3/ZnO/TiO_2$ composite film electrodes towards pentachlorophenol degradation, Phys. Chem. Chem. Phys. 6 (2004) 659–664.
[23] Y.F. Guo, X. Quan, N. Liu, H.M. Zhao, S. Chen, High photocatalytic capability of self-assembled nanoporous WO_3 with preferential orientation of (0 0 2) planes, Environ. Sci. Technol. 41 (2007) 4422–4427.
[24] J. Arana, J.M. Dona-Rodriguez, J.A.H. Melian, E.T. Rendon, O.G. Diaz, Role of Pd and Cu in gas-phase alcohols photocatalytic degradation with doped TiO_2, J. Photochem. Photobiol. A 174 (2005) 7–14.
[25] C. Belver, M.J. Lopez-Munoz, J.M. Coronado, J. Soria, Palladium enhanced resistance to deactivation of titanium dioxide during the photocatalytic oxidation of toluene vapors, Appl. Catal. B 46 (2003) 497–509.
[26] Z.Y. Sheng, Z.B. Wu, Y. Liu, H.Q. Wang, Gas-phase photocatalytic oxidation of NO over palladium modified TiO_2 catalysts, Catal. Commun. 9 (2008) 1941–1944.
[27] M.C. Yan, F. Chen, J.L. Zhang, M. Anpo, Preparation of controllable crystalline titania and study on the photocatalytic properties, J. Phys. Chem. B 109 (2005) 8673–8678.
[28] M. Hirano, C. Nakahara, K. Ota, O. Tanaike, M. Inagaki, Photoactivity and phase stability of ZrO_2-doped anatase-type TiO_2 directly formed as nanometer-sized particles by hydrolysis under hydrothermal conditions, J. Solid State Chem. 170 (2003) 39–47.
[29] S.Y. Chae, M.K. Park, S.K. Lee, T.Y. Kim, S.K. Kim, W.I. Lee, Preparation of size-controlled TiO_2 nanoparticles and derivation of optically transparent photocatalytic film, Chem. Mater. 15 (2003) 3326–3331.
[30] A.K. Datye, J. Bravo, T.R. Nelson, P. Atanasova, M. Lyubovsky, L. Pfefferle, Catalyst microstructure and methane oxidation reactivity during the Pd↔PdO transformation on alumina supports, Appl. Catal. A 198 (2000) 179–196.
[31] Z. Zhang, G. Mestl, H. Knozinger, W.M.H. Sachtler, Effects of calcination program and rehydration on palladium dispersion in zeolites NaY and 5A, Appl. Catal. A 89 (1992) 155–168.
[32] W.F. Zhang, M.S. Zhang, Z. Yin, Q. Chen, Photoluminescence in anatase titanium dioxide nanocrystals, Appl. Phys. B 70 (2000) 261–265.
[33] J.C. Yu, J.G. Yu, W.K. Ho, Z.T. Jiang, L.Z. Zhang, Effects of F^- doping on the photocatalytic activity and microstructures of nanocrystalline TiO_2 powders, Chem. Mater. 14 (2002) 3808–3816.
[34] J.G. Yu, H.G. Yu, B. Cheng, X.J. Zhao, J.C. Yu, W.K. Ho, The effect of calcination temperature on the surface microstructure and photocatalytic activity of TiO_2 thin films prepared by liquid phase deposition, J. Phys. Chem. B 107 (2003) 13871–13879.
[35] A. Fujishima, T.N. Rao, D.A. Tryk, Titanium dioxide photocatalysis, J. Photochem. Photobiol. C 1 (2000) 1–21.
[36] R. Nakamura, A. Imanishi, K. Murakoshi, Y. Nakato, In situ FTIR studies of primary intermediates of photocatalytic reactions on nanocrystalline TiO_2 films in contact with aqueous solutions, J. Am. Chem. Soc. 125 (2003) 7443–7450.
[37] R. Nakamura, Y. Nakato, Primary intermediates of oxygen photoevolution reaction on TiO_2 (rutile) particles, revealed by in situ FTIR absorption and photoluminescence measurements, J. Am. Chem. Soc. 126 (2004) 1290–1298.
[38] R. Nakamura, N. Ohashi, A. Imanishi, T. Osawa, Y. Matsumoto, H. Koinuma, Y. Nakato, Crystal-face dependences of surface band edges and hole reactivity, revealed by preparation of essentially atomically smooth and stable (1 1 0) and (1 0 0) *n*-TiO_2 (rutile) surfaces, J. Phys. Chem. B 109 (2005) 1648–1651.
[39] R. Nakamura, T. Okamura, N. Ohashi, A. Imanishi, Y. Nakato, Molecular mechanisms of photoinduced oxygen evolution, PL emission, and surface roughening at atomically smooth (1 1 0) and (1 0 0) *n*-TiO_2 (rutile) surfaces in aqueous acidic solutions, J. Am. Chem. Soc. 127 (2005) 12975–12983.
[40] T.A. Egerton, I.R. Tooley, Effect of changes in TiO_2 dispersion on its measured photocatalytic activity, J. Phys. Chem. B 108 (2004) 5066–5072.
[41] T. Hirakawa, H. Kominami, B. Ohtani, Y. Nosaka, Mechanism of photocatalytic production of active oxygens on highly crystalline TiO_2 particles by means of chemiluminescent probing and ESR spectroscopy, J. Phys. Chem. B 105 (2001) 6993–6999.
[42] T. Ohno, K. Sarukawa, K. Tokieda, M. Matsumura, Morphology of a TiO_2 photocatalyst (Degussa, P-25) consisting of anatase and rutile crystalline phases, J. Catal. 203 (2001) 82–86.
[43] S. Roy, M.S. Hegde, N. Ravishankar, G. Madras, Creation of redox adsorption sites by Pd^{2+} ion substitution in nanoTiO_2 for high photocatalytic activity of CO oxidation, NO reduction, and NO decomposition, J. Phys. Chem. C 111 (2007) 8153–8160.